

Electronic Supplementary Information (ESI) for:

On-Surface Synthesis of Heptacene and its Interaction with a Metal Surface

Malte Zugermeier^a, Manuel Gruber^b, Martin Schmid^a, Benedikt P. Klein^a, Lukas Ruppenthal^a, Philipp Müller^a, Ralf Einholz^c, Wolfgang Hieringer^d, Richard Berndt^b, Holger F. Bettinger^c, J. Michael Gottfried^{a*}

^a Philipps-Universität Marburg, Fachbereich Chemie, Hans-Meerwein-Str. 4, 35032 Marburg, Germany, michael.gottfried@chemie.uni-marburg.de

^b Christian-Albrechts-Universität zu Kiel, Institut für Experimentelle und Angewandte Physik, Leibnizstraße 19, 24098 Kiel, Germany

^c Universität Tübingen, Institut für Organische Chemie, Auf der Morgenstelle 18, 72076 Tübingen, Germany

^d Lehrstuhl für Theoretische Chemie, Friedrich-Alexander-Universität Erlangen-Nürnberg, Egerlandstr. 3, 91058 Erlangen, Germany

1. X-ray Photoelectron Spectroscopy

To monitor the surface-assisted didecarbonylation reaction of 7,16-dihydro-7,16-ethanoheptacene-19,20-dione (DEH) on Ag(111), X-ray photoelectron spectra of the C1s (Figure S1) and O1s regions (Figure S2) were recorded in a temperature range of 300 to 700 K.

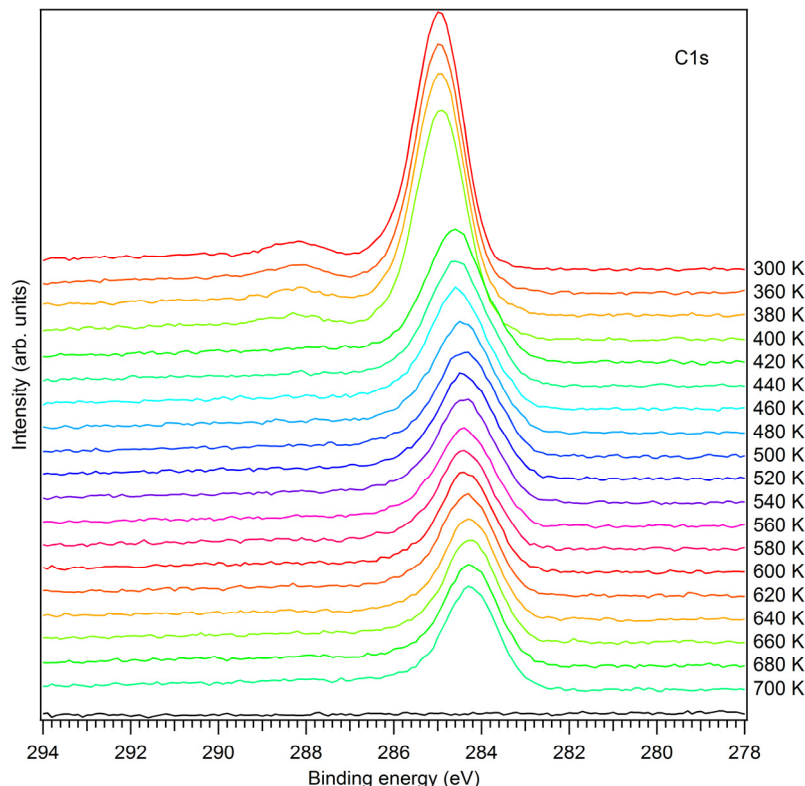


Figure S1. Temperature-programmed C1s XP spectra showing the transition of 7,16-dihydro-7,16-ethanoheptacene-19,20-dione (DEH, initial coverage 2 ML) to heptacene.

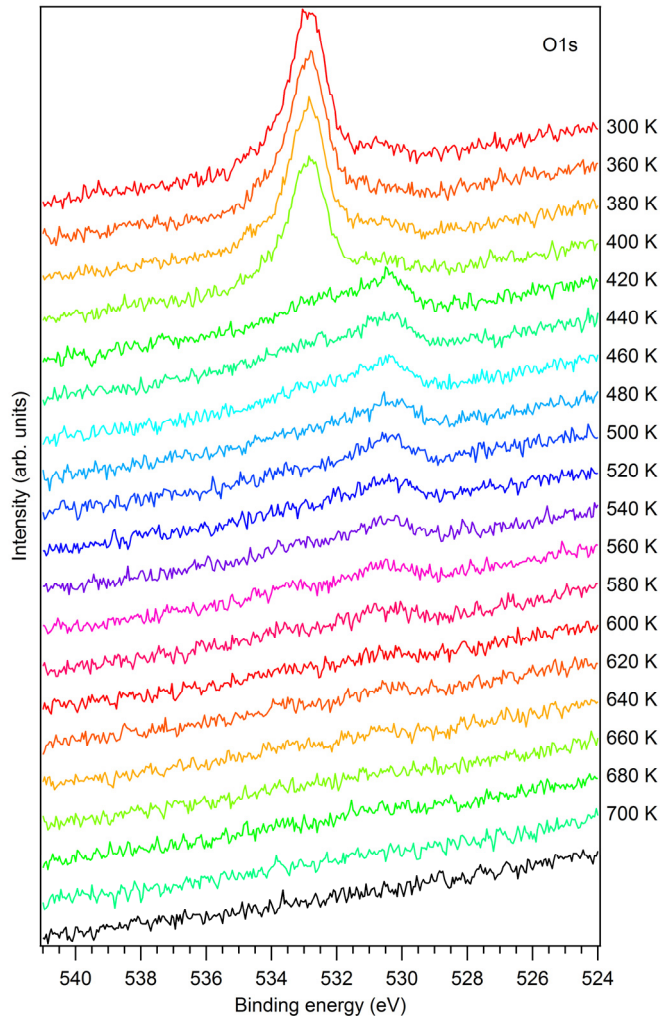


Figure S2. Temperature-programmed O1s XP spectra showing the transition of 7,16-dihydro-7,16-ethanoheptacene-19,20-dione (DEH, initial coverage 2 ML) to heptacene.

The O1s spectrum of 7,16-dihydro-7,16-ethanoheptacene-19,20-dione exhibits two different oxygen species at room temperature. The peak at higher binding energy is attributed to the oxygen species at the diketone bridge of 7,16-dihydro-7,16-ethanoheptacene-19,20-dione. The species at lower binding energy, visible as a small shoulder of the major feature, is an unknown impurity (possibly chemisorbed oxygen). Both features are present in monolayer as well as in multilayer spectra (Figure S3).

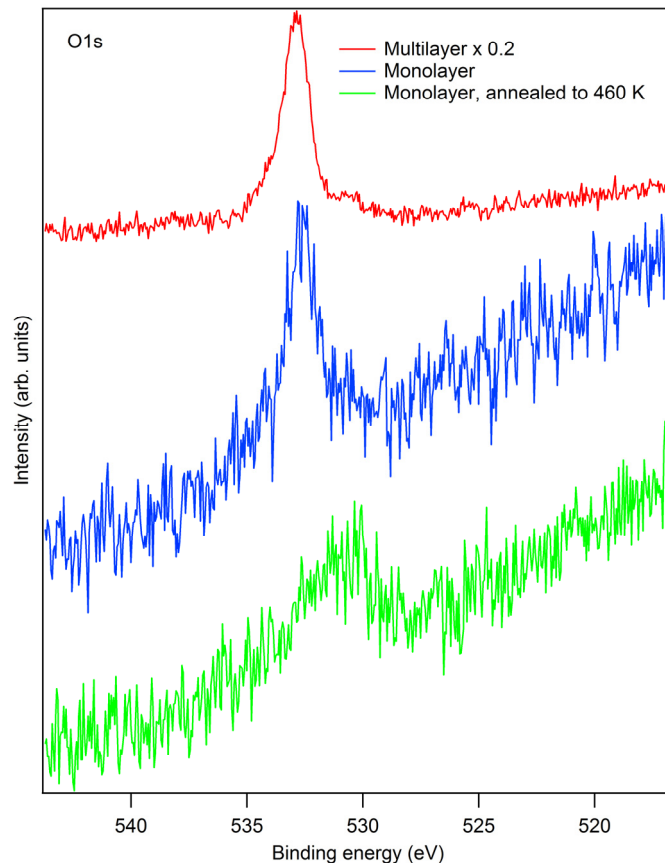


Figure S3. Comparison of multilayer and monolayer O1s XP spectra of 7,16-dihydro-7,16-ethanoheptacene-19,20-dione (DEH) at room temperature and monolayer spectrum after annealing to 460 K.

2. Near-Edge X-ray Absorption Fine Structure (NEXAFS) Spectroscopy

A quantitative analysis is based on Fermi's "Golden Rule", according to which the intensity, I_{if} , of a dipole transition depends on the orientation of the electric field vector, \vec{E} , relative to the dipole matrix element, $\langle f | \vec{R} | i \rangle$. If the initial state, i , is the K shell, this dipole matrix element points in the same direction as the p-component in the final state orbital, f , on the excited atom. In this case, the polarization dependence of I_{if} is given by the angle δ between the direction of the electric field vector and the direction \vec{T} of the largest amplitude of the final state orbital:¹

$$I_{if} \propto |\vec{E} \cdot \langle f | \vec{R} | i \rangle|^2 \propto |\vec{E} \cdot \vec{T}|^2 \propto \cos^2 \delta \quad \text{Equation (1)}$$

To determine the orientation of the molecule relative to the surface, it is more convenient to use the angle between \vec{T} and the surface normal, α , and the angle between \vec{E} and the surface normal, ε , as shown in Figure 3. With these angles, the intensity of the π^* resonance, I_{π^*} , for a substrate with threefold symmetry is given by:¹

$$I_{\pi^*} \propto P \cos^2(\varepsilon) \left(\cos^2(\alpha) + \frac{1}{2P} \tan^2(\varepsilon) \sin^2(\alpha) \right) \quad \text{Equation (2)}$$

The degree of polarization, P , for the beamline used in this experiment is $P = 0.91$. For fitting the experimental data a normalization factor b has to be introduced.

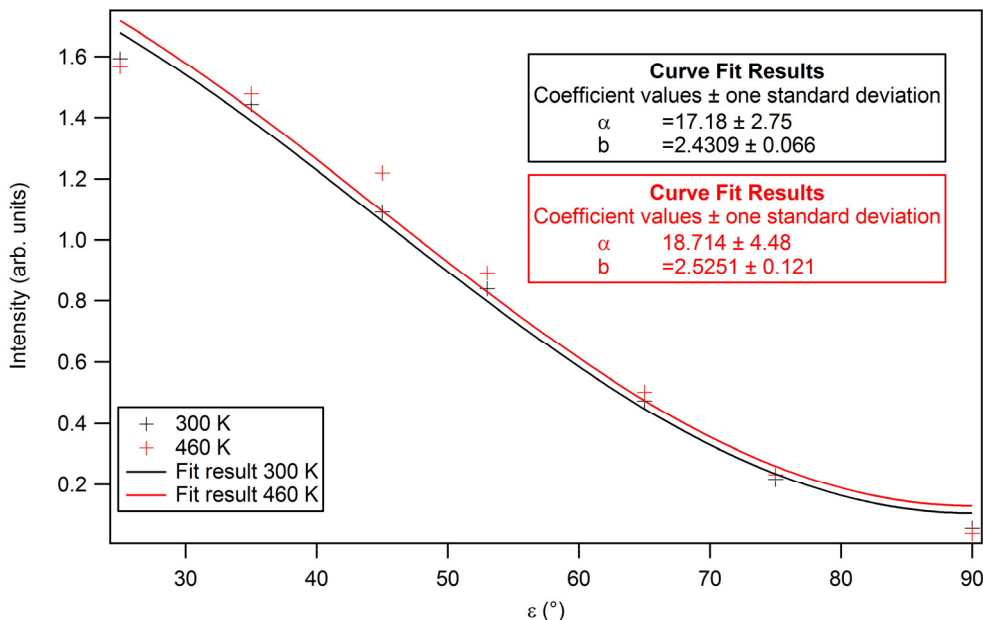


Figure S4. π^* peak intensities at 284.5 eV as a function of the X-ray incidence angle ε , and the corresponding fits using Equation (2) for a degree of polarization of $P = 0.91$. The parameter b was introduced into the equation as a normalization factor.

3. Scanning Tunneling Microscopy

Low-temperature scanning tunneling microscopy after annealing of 7,16-dihydro-7,16-ethanoheptacene-19,20-dione (DEH) on Ag(111) to 460 K shows predominantly immobile features attributed to individual heptacene molecules. In addition, mobile features in the form of stripes are observed, which most likely are residual DEH molecules. The features in Figure S5 were counted to estimate the ratio between reacted heptacene and unreacted diketone precursor molecules. Each stripe was attributed to one precursor molecule. The area of $100 \times 100 \text{ nm}^2$ exhibits 29 mobile molecules, 93 immobile molecules. The relatively high percentage of mobile features (ca. 1/4) represents an upper limit, because the diffusion traces most likely continue outside the frame shown in Figure S5. This means that they belong to a larger area than the immobile heptacene-related features. Furthermore, some mobile features are most likely the result of a multiple tip effect, which is absent for the immobile feature due to their distinctly lower height. If only the mobile features with an apparent height of 360 pm are counted, their percentage decreases to ~14% (15 mobile features). Again, this value represents an upper limit.

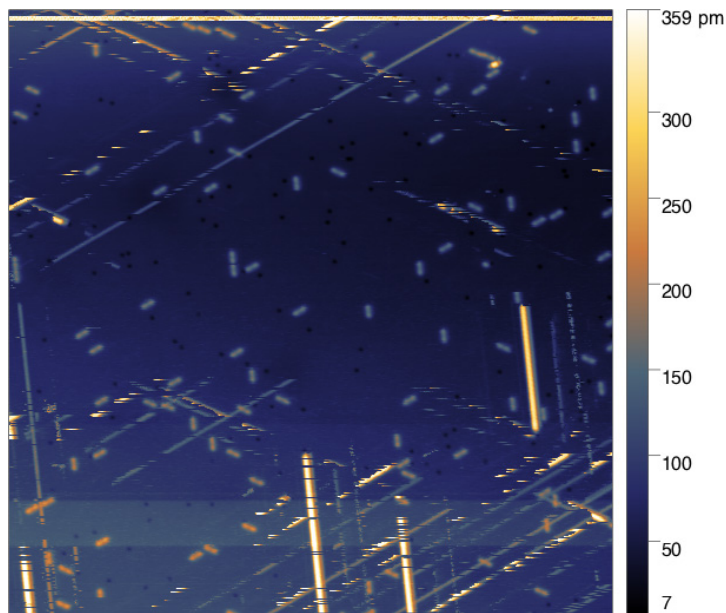


Figure S5. LT-STM image (4K) of heptacene and residual DEH molecules after room temperature adsorption onto Ag(111) and annealing to 460 K. Image size: $100 \times 100 \text{ nm}^2$. Imaging parameters: 1.3 V, 2 pA.

STM images of immobile DEH molecules were not achieved by LT-STM due to their mobility and the need for low coverages to improve the imaging quality by tip pulsing on the bare Ag(111) substrate. Therefore, complementary studies at coverages close to a monolayer were performed with a variable-temperature STM at 150 K. The closer packing of the molecules at these higher coverages enabled the imaging of the precursor molecules, even though mobility issues and lacking long-range order made the imaging still very difficult. Central protrusions are distinguishable at the center of the molecules, which most probably correspond to the diketone bridge (Figure S6).

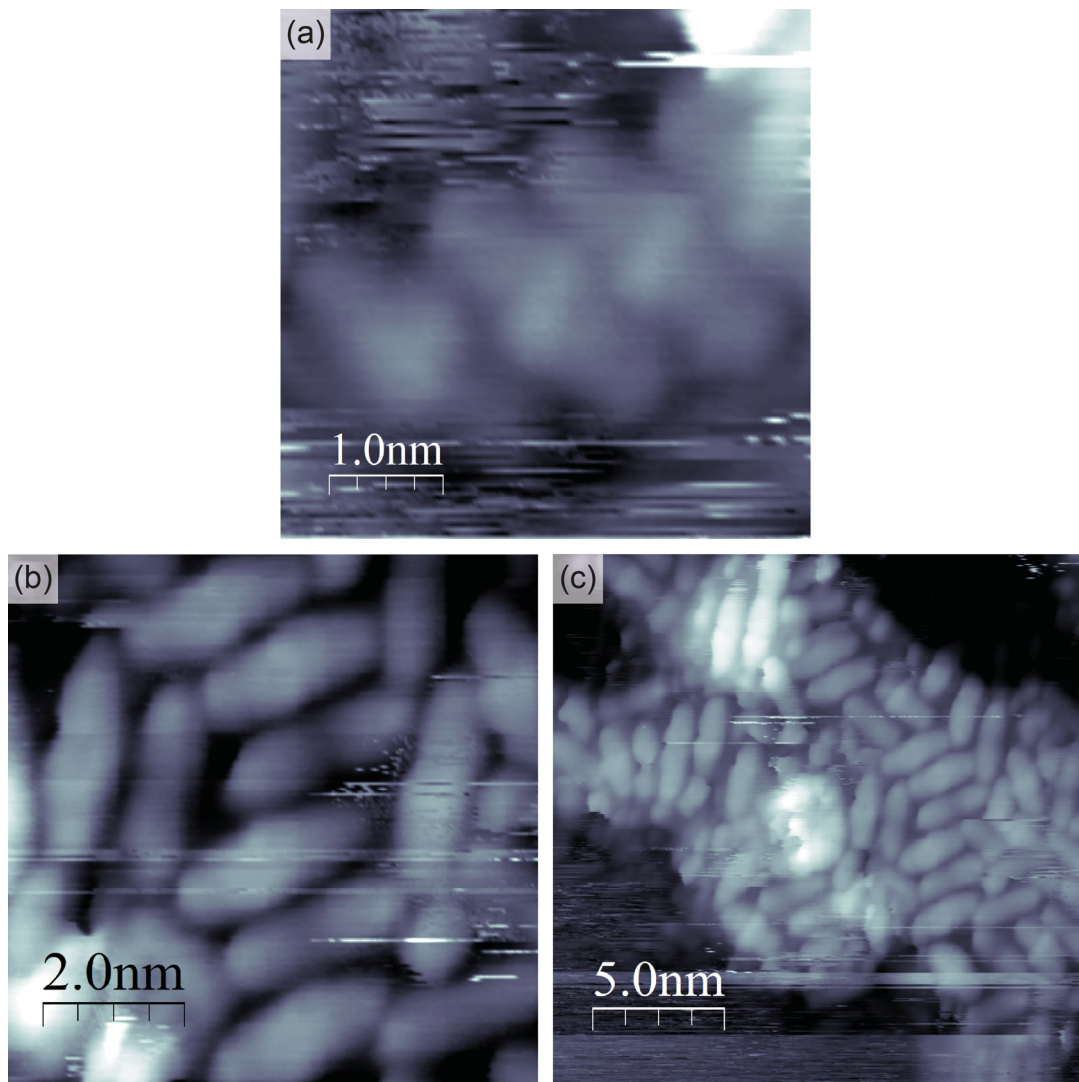


Figure S6. VT-STM images of DEH after room temperature adsorption onto Ag(111). Imaging parameters: (a) 1.24 V, 0.26 nA; (b) 1.24 V, 0.26 nA; (c) 1.24 V, 0.25 nA. Despite the higher coverage, imaging was still difficult due to high mobility and limited tendency for the formation of a long-range ordered structure.

After annealing DEH on Ag(111) 460 K, the molecules appear less mobile and evenly distributed on the substrate compared to the small immobilized domains of the DEH. Molecules with central protrusions now only occur in a low amount (Figure S7). It can be concluded that a predominant part of the DEH molecules was converted to heptacene.

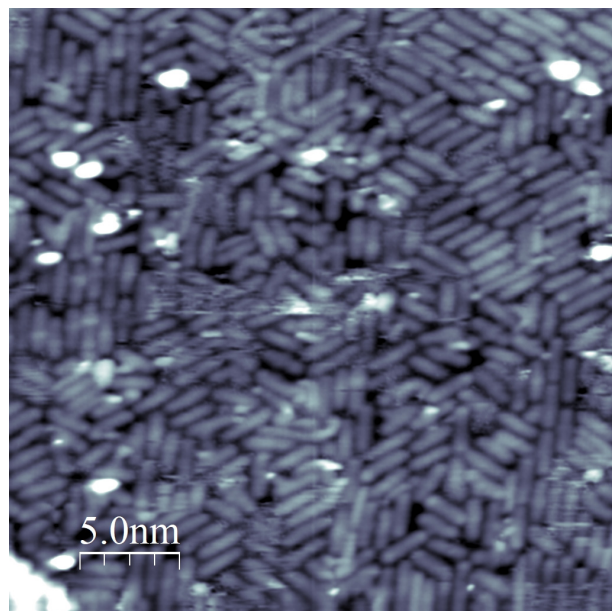


Figure S7. VT-STM image of heptacene molecules after annealing to 460 K. Imaging parameters: -1.54 V, -0.14 nA.

4. Density Functional Theory (DFT) Calculations

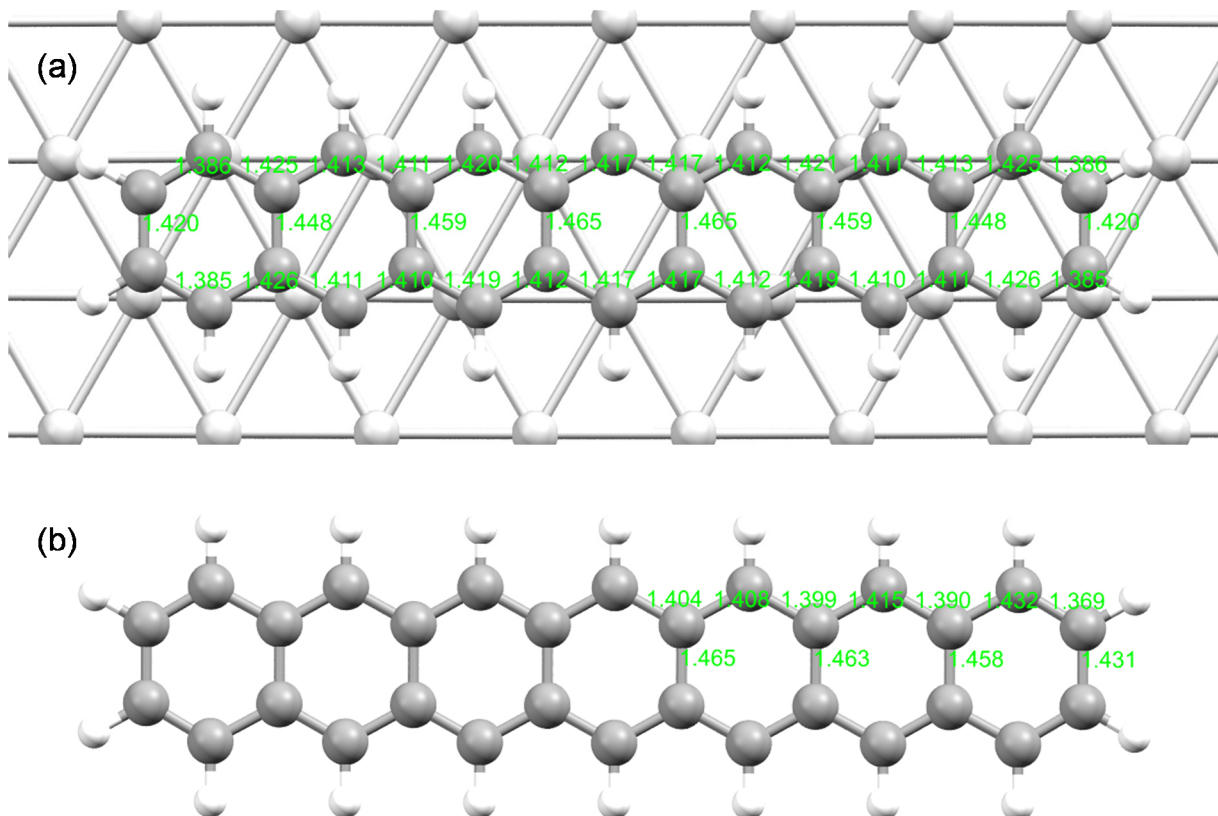


Figure S8. C-C bond lengths in Å in the optimized geometry of (a) heptacene on Ag(111) and (b) the free heptacene molecule.

Atomic coordinates of the optimized geometry of heptacene on Ag(111), VASP POSCAR format; see the main paper for computational details and a graphical representation (Figure 5), as well as Figure S8a.

Heptacene on Ag(111)

1.0

+26.1587436186 +0.0000000000 +0.0000000000
+0.0000000000 +10.0685051132 +0.0000000000
+0.0000000000 +0.0000000000 +27.2195082420

C H Ag

30 18 144

Selective

Cartesian

+2.9715345483 +6.9207476569 +9.9634327704 TTT
+2.9765788974 +5.5011743535 +9.9782410255 TTT
+4.1784046729 +4.8126968845 +9.9576619150 TTT
+5.4263629817 +5.5014111840 +9.9138313679 TTT
+5.4201238224 +6.9495020266 +9.9091166233 TTT
+4.1653183849 +7.6245361548 +9.9284259092 TTT
+6.6631494117 +4.8247122690 +9.8611043120 TTT
+7.8967094430 +5.5073606858 +9.8234338686 TTT
+7.8918953757 +6.9660003091 +9.8314167330 TTT
+6.6523755806 +7.6387259215 +9.8588480294 TTT
+9.1425702795 +4.8320625006 +9.7540944632 TTT
+10.3799409293 +5.5112332911 +9.7523116244 TTT
+10.3771486372 +6.9760170520 +9.7752734415 TTT
+9.1365035973 +7.6494327893 +9.7930193439 TTT
+11.6253320734 +4.8369765561 +9.7097201203 TTT
+12.8688490887 +5.5147559806 +9.7526934913 TTT
+12.8673506271 +6.9795562981 +9.7750355550 TTT
+11.6212187116 +7.6545480216 +9.7694921410 TTT
+14.1081348637 +4.8390925076 +9.7552932701 TTT
+15.3520959705 +5.5180082201 +9.8244694156 TTT
+15.3526801006 +6.9766534799 +9.8307092249 TTT
+14.1060156150 +7.6565475351 +9.7917739988 TTT
+16.5875788360 +4.8389349602 +9.8639748199 TTT
+17.8223395394 +5.5192530128 +9.9168132638 TTT
+17.8243887427 +6.9672980189 +9.9092867794 TTT
+16.5902189886 +7.6529972074 +9.8572609612 TTT
+19.0722809972 +4.8342597460 +9.9632711741 TTT
+20.2719608585 +5.5262580120 +9.9831321344 TTT
+20.2729757614 +6.9457648239 +9.9646598973 TTT
+19.0772055622 +7.6460433670 +9.9276319857 TTT
+2.0221505256 +7.4593392447 +9.9943765217 TTT
+2.0329317388 +4.9559979112 +10.0350794303 TTT
+4.1863960958 +3.7200520000 +9.9798234438 TTT
+4.1585867947 +8.7172759025 +9.9407702510 TTT
+6.6669296133 +3.7311613577 +9.8801839980 TTT
+6.6456648860 +8.7320255890 +9.8858998842 TTT
+9.1455470311 +3.7390855743 +9.7913556914 TTT

+9.1330972460 +8.7419847230 +9.8411223713 T T T
 +11.6268273863 +3.7443639811 +9.7570250106 T T T
 +11.6196637400 +8.7468274843 +9.8250838078 T T T
 +14.1081329705 +3.7461507588 +9.7934716312 T T T
 +14.1063301311 +8.7491689909 +9.8388365387 T T T
 +16.5868365706 +3.7454412693 +9.8849504362 T T T
 +16.5938066889 +8.7463742336 +9.8827820752 T T T
 +19.0675080570 +3.7416586573 +9.9875766500 T T T
 +21.2172574613 +4.9840408296 +10.0411538241 T T T
 +21.2207406346 +7.4872933743 +9.9944612851 T T T
 +19.0807501418 +8.7388594831 +9.9374587332 T T T
 +0.00000000000 +0.00000000000 +0.00000000000 F F F
 +2.9065270688 +0.00000000000 +0.00000000000 F F F
 +5.8130541375 +0.00000000000 +0.00000000000 F F F
 +8.7195812062 +0.00000000000 +0.00000000000 F F F
 +11.6261082749 +0.00000000000 +0.00000000000 F F F
 +14.5326353437 +0.00000000000 +0.00000000000 F F F
 +17.4391624124 +0.00000000000 +0.00000000000 F F F
 +20.3456894811 +0.00000000000 +0.00000000000 F F F
 +23.2522165498 +0.00000000000 +0.00000000000 F F F
 +1.4532635343 +2.5171262783 +0.00000000000 F F F
 +4.3597906031 +2.5171262783 +0.00000000000 F F F
 +7.2663176718 +2.5171262783 +0.00000000000 F F F
 +10.1728447406 +2.5171262783 +0.00000000000 F F F
 +13.0793718092 +2.5171262783 +0.00000000000 F F F
 +15.9858988780 +2.5171262783 +0.00000000000 F F F
 +18.8924259467 +2.5171262783 +0.00000000000 F F F
 +21.7989530155 +2.5171262783 +0.00000000000 F F F
 +24.7054800842 +2.5171262783 +0.00000000000 F F F
 +0.00000000000 +5.0342525566 +0.00000000000 F F F
 +2.9065270688 +5.0342525566 +0.00000000000 F F F
 +5.8130541375 +5.0342525566 +0.00000000000 F F F
 +8.7195812062 +5.0342525566 +0.00000000000 F F F
 +11.6261082749 +5.0342525566 +0.00000000000 F F F
 +14.5326353437 +5.0342525566 +0.00000000000 F F F
 +17.4391624124 +5.0342525566 +0.00000000000 F F F
 +20.3456894811 +5.0342525566 +0.00000000000 F F F
 +23.2522165498 +5.0342525566 +0.00000000000 F F F
 +1.4532635343 +7.5513788349 +0.00000000000 F F F
 +4.3597906031 +7.5513788349 +0.00000000000 F F F
 +7.2663176718 +7.5513788349 +0.00000000000 F F F
 +10.1728447406 +7.5513788349 +0.00000000000 F F F
 +13.0793718092 +7.5513788349 +0.00000000000 F F F
 +15.9858988780 +7.5513788349 +0.00000000000 F F F
 +18.8924259467 +7.5513788349 +0.00000000000 F F F
 +21.7989530155 +7.5513788349 +0.00000000000 F F F
 +24.7054800842 +7.5513788349 +0.00000000000 F F F
 +1.4532635343 +0.8390420928 +2.3731694140 F F F
 +4.3597906031 +0.8390420928 +2.3731694140 F F F
 +7.2663176718 +0.8390420928 +2.3731694140 F F F
 +10.1728447406 +0.8390420928 +2.3731694140 F F F
 +13.0793718092 +0.8390420928 +2.3731694140 F F F

+15.9858988780 +0.8390420928 +2.3731694140 F F F
 +18.8924259467 +0.8390420928 +2.3731694140 F F F
 +21.7989530155 +0.8390420928 +2.3731694140 F F F
 +24.7054800842 +0.8390420928 +2.3731694140 F F F
 +0.0000000000 +3.3561683711 +2.3731694140 F F F
 +2.9065270688 +3.3561683711 +2.3731694140 F F F
 +5.8130541375 +3.3561683711 +2.3731694140 F F F
 +8.7195812062 +3.3561683711 +2.3731694140 F F F
 +11.6261082749 +3.3561683711 +2.3731694140 F F F
 +14.5326353437 +3.3561683711 +2.3731694140 F F F
 +17.4391624124 +3.3561683711 +2.3731694140 F F F
 +20.3456894811 +3.3561683711 +2.3731694140 F F F
 +23.2522165498 +3.3561683711 +2.3731694140 F F F
 +1.4532635343 +5.8732946494 +2.3731694140 F F F
 +4.3597906031 +5.8732946494 +2.3731694140 F F F
 +7.2663176718 +5.8732946494 +2.3731694140 F F F
 +10.1728447406 +5.8732946494 +2.3731694140 F F F
 +13.0793718092 +5.8732946494 +2.3731694140 F F F
 +15.9858988780 +5.8732946494 +2.3731694140 F F F
 +18.8924259467 +5.8732946494 +2.3731694140 F F F
 +21.7989530155 +5.8732946494 +2.3731694140 F F F
 +24.7054800842 +5.8732946494 +2.3731694140 F F F
 +0.0000000000 +8.3904209277 +2.3731694140 F F F
 +2.9065270688 +8.3904209277 +2.3731694140 F F F
 +5.8130541375 +8.3904209277 +2.3731694140 F F F
 +8.7195812062 +8.3904209277 +2.3731694140 F F F
 +11.6261082749 +8.3904209277 +2.3731694140 F F F
 +14.5326353437 +8.3904209277 +2.3731694140 F F F
 +17.4391624124 +8.3904209277 +2.3731694140 F F F
 +20.3456894811 +8.3904209277 +2.3731694140 F F F
 +23.2522165498 +8.3904209277 +2.3731694140 F F F
 +26.1549158073 +1.6747710865 +4.6992713074 T T T
 +2.8968659932 +1.6798264779 +4.6923231003 T T T
 +5.8043373070 +1.6819318243 +4.6849640684 T T T
 +8.7143741559 +1.6788335226 +4.6832000666 T T T
 +11.6262309013 +1.6789876650 +4.6823808545 T T T
 +14.5380544364 +1.6793385567 +4.6832829422 T T T
 +17.4478078619 +1.6825983182 +4.6850508416 T T T
 +20.3550319729 +1.6804408186 +4.6923832403 T T T
 +23.2555272526 +1.6749717927 +4.6993438910 T T T
 +1.4493407232 +4.1938288091 +4.7051739363 T T T
 +4.3469778750 +4.1961476593 +4.7052451975 T T T
 +7.2600059055 +4.1924909481 +4.6930044854 T T T
 +10.1702859418 +4.1925974491 +4.6911423782 T T T
 +13.0821797311 +4.1928047327 +4.6912662386 T T T
 +15.9922942539 +4.1931271544 +4.6933932140 T T T
 +18.9049065227 +4.1967070090 +4.7054642011 T T T
 +21.8025329608 +4.1942018237 +4.7052291027 T T T
 +24.7052790000 +4.1907923295 +4.6951517628 T T T
 +26.1553810141 +6.7086959054 +4.6982862768 T T T
 +2.9031442972 +6.7045735185 +4.7093449913 T T T
 +5.8082279398 +6.7108203874 +4.7095500131 T T T

+8.7158619911 +6.7084889039 +4.7140077400 TTT
 +11.6260801002 +6.7083476421 +4.7148102776 TTT
 +14.5362782039 +6.7087672802 +4.7139374790 TTT
 +17.4439999216 +6.7112637714 +4.7095641420 TTT
 +20.3489443773 +6.7050818402 +4.7092101696 TTT
 +23.2553992666 +6.7088184116 +4.6982696335 TTT
 +1.4509967174 +9.2267838096 +4.6981589188 TTT
 +4.3541843402 +9.2327158776 +4.6950521712 TTT
 +7.2624764436 +9.2304956855 +4.6960260876 TTT
 +10.1713215405 +9.2270714451 +4.6972558671 TTT
 +13.0809572838 +9.2273129026 +4.6971343561 TTT
 +15.9897084039 +9.2310839810 +4.6956879822 TTT
 +18.8979681299 +9.2333249276 +4.6948397451 TTT
 +21.8010846707 +9.2270669480 +4.6980888191 TTT
 +24.7053777852 +9.2267761359 +4.7003526198 TTT
 +26.1538546804 +10.0657453729 +7.0560111849 TTT
 +2.8913486667 +0.0090663236 +7.0455919542 TTT
 +5.8027238353 +0.0150710169 +7.0395014662 TTT
 +8.7121373895 +0.0134364685 +7.0382871948 TTT
 +11.6260332151 +0.0139512357 +7.0369746088 TTT
 +14.5399437473 +0.0142591916 +7.0379543357 TTT
 +17.4493324255 +0.0164465211 +7.0388339768 TTT
 +20.3608562114 +0.0102683613 +7.0451242047 TTT
 +23.2568606243 +10.0661521216 +7.0559338052 TTT
 +1.4428473986 +2.5107102785 +7.0550194972 TTT
 +4.3487983716 +2.4966771487 +7.0405182681 TTT
 +7.2555728381 +2.4876174746 +7.0324454337 TTT
 +10.1678163967 +2.4799801273 +7.0263126754 TTT
 +13.0843784195 +2.4804725203 +7.0265129441 TTT
 +15.9965109618 +2.4890091343 +7.0331345671 TTT
 +18.9031210099 +2.4981707527 +7.0412315865 TTT
 +21.8088862531 +2.5116823125 +7.0554435856 TTT
 +24.7052732490 +2.5163832790 +7.0540975957 TTT
 +26.1508700767 +5.0326726926 +7.0513813033 TTT
 +2.8870080266 +5.0188847080 +7.0656482587 TTT
 +5.8024846797 +5.0090886687 +7.0159643567 TTT
 +8.7080353286 +4.9921011665 +7.0101398242 TTT
 +11.6261500041 +4.9854862202 +7.0022013231 TTT
 +14.5441470627 +4.9930886990 +7.0108003371 TTT
 +17.4496821866 +5.0106266236 +7.0172151742 TTT
 +20.3645970455 +5.0201324221 +7.0659498348 TTT
 +23.2594850650 +5.0329859430 +7.0515627642 TTT
 +1.4388270455 +7.5540507117 +7.0403825151 TTT
 +4.3493978498 +7.5768861467 +7.0221845487 TTT
 +7.2637555080 +7.5734015224 +7.0265505191 TTT
 +10.1730816434 +7.5717743612 +7.0269193989 TTT
 +13.0787892562 +7.5723003124 +7.0266419374 TTT
 +15.9883607905 +7.5746541567 +7.0257555909 TTT
 +18.9029331321 +7.5783100420 +7.0218289895 TTT
 +21.8132893832 +7.5546526726 +7.0403248894 TTT
 +24.7053609794 +7.5486711114 +7.0597890942 TTT

References

1. Stöhr, J. *NEXAFS Spectroscopy*. Corr. 2. printing ed.; Springer-Verlag Berlin Heidelberg: 1996.